International Journal of Geo-Information

MDPI

Article

Applying Dynamic Human Activity to Disentangle Property Crime Patterns in London during the Pandemic: An Empirical Analysis Using Geo-Tagged Big Data

Tongxin Chen [1,*], Kate Bowers [2] and Tao Cheng [1]

[1] SpaceTimeLab for Big Data Analytics, Department of Civil, Environmental and Geomatic Engineering, University College London, Gower Street, London WC1E 6BT, UK
[2] Department of Security and Crime Science, University College London, Tavistock Square, London WC1H 9EZ, UK; kate.bowers@ucl.ac.uk
* Correspondence: tongxin.chen.18@ucl.ac.uk

Abstract: This study aimed to evaluate the relationships between different groups of explanatory variables (i.e., dynamic human activity variables, static variables of social disorganisation and crime generators, and combinations of both sets of variables) and property crime patterns across neighbourhood areas of London during the pandemic (from 2020 to 2021). Using the dynamic human activity variables sensed from mobile phone GPS big data sets, three types of 'Least Absolute Shrinkage and Selection Operator' (LASSO) regression models (i.e., static, dynamic, and static and dynamic) differentiated into explanatory variable groups were developed for seven types of property crime. Then, the geographically weighted regression (GWR) model was used to reveal the spatial associations between distinct explanatory variables and the specific type of crime. The findings demonstrated that human activity dynamics impose a substantially stronger influence on specific types of property crimes than other static variables. In terms of crime type, theft obtained particularly high relationships with dynamic human activity compared to other property crimes. Further analysis revealed important nuances in the spatial associations between property crimes and human activity across different contexts during the pandemic. The result provides support for crime risk prediction that considers the impact of dynamic human activity variables and their varying influences in distinct situations.

Keywords: mobile phone GPS data; human mobility; crime risk; urban mobility; urban vibrancy; COVID; pandemic

Citation: Chen, T.; Bowers, K.; Cheng, T. Applying Dynamic Human Activity to Disentangle Property Crime Patterns in London during the Pandemic: An Empirical Analysis Using Geo-Tagged Big Data. *ISPRS Int. J. Geo-Inf.* **2023**, *12*, 488. https://doi.org/10.3390/ijgi12120488

Academic Editors: Wolfgang Kainz and Hartwig H. Hochmair

Received: 10 October 2023
Revised: 27 November 2023
Accepted: 3 December 2023
Published: 6 December 2023

1. Introduction

In response to the COVID-19 outbreak, local governments implemented social distancing measures (e.g., stay-at-home, national lockdowns) to reduce virus transmissions, consequentially causing a tremendous disruption of citizens' daily routine activity in global cities [1,2]. Substantial criminological studies have widely reported that crime patterns have been affected by human activity shifting due to the COVID-19 social policies. The preliminary studies addressed the property-related drops in crime during the early COVID-19 outbreak months in 2020, such as observable reductions in residential burglary, theft, robbery, and shoplifting [3–9]. As time elapsed and the pandemic restriction policies lifted, crime recovery following reduction was portrayed as 'U-shaped' crime patterns as human activities approached the pre-pandemic level [10–12].

Several pandemic-related crime studies, using the pandemic as a natural experiment, have demonstrated that property crime variations are prominently affected by human routine dynamics in cities or regions [8,13,14]. To date, as is highlighted by our literature review below, there has been less focus on the relationship between the dynamic rhythms of population activity and property crime patterns in local neighbourhoods/communities

during the pandemic. Considering the daily routine activity in populations in space and time, it would be helpful to understand the crime shifting in neighbourhoods during the pandemic by comprehensively examining the effects of dynamic human activity variables intertwined with other neighbourhood characteristics. The current study aimed to fill this gap by addressing three research questions: (1) How do dynamic human activity patterns and /or static neighbourhood characteristics vary in terms of their impacts on property crime levels? (2) Do such impacts vary by type of property crime? and (3) Which situation-specific dynamic human activity levels show the strongest associations with a specific type of property crime?

To answer these research questions, we implemented our empirical analytics on seven types of property crimes (i.e., bicycle theft, burglary, criminal damage and arson, robbery, shoplifting, theft from a person, and vehicle crime) in the neighbourhoods of London, U.K., from 2020 to 2021. We first measured the dynamic human activity variables characterised by the population's weekly or daily routines (i.e., early morning, morning, midday, afternoon, and evening of weekdays or weekends) based on footfalls detected from anonymous mobile phone GPS data. Then, we identified the associations between dynamic activity variables, static neighbourhood characteristic (socioeconomic and place) variables, and property crime rates in the trained LASSO regression models. Three types of models varying in the input variable groups (i.e., static, dynamic, and static and dynamic) were then compared to identify the distinctive impact of dynamic human activity on crime patterns. Finally, a deeper spatial analysis was undertaken for a particular crime type (theft from a person) to further explore the nuances between dynamic activity patterns and crime in different contexts.

2. Review of Related Works

2.1. Theoretical Approaches and Crime Shifting during the COVID-19 Pandemic

Current COVID-19 and crime research mainly utilises crime opportunity concepts originally from routine activity theory (RAT) [15] and crime pattern theory (CPT) [16] to explain the crime shift driven by human activities (e.g., mobility variations) during the pandemic. RAT suggests that crime opportunity arises when the motivated offenders and suitable targets/victims coincide in the absence of capable guardianship [17,18]. In applying this idea, it is useful to consider that the interactions between potential offenders and victims in the population's daily activities are shaped by urban places, neighbourhoods, and built environments [19]. Further, according to CPT, there are places with high concentrations of population visits that provide particularly high levels of opportunities, which are known as crime generators [20]. Accordingly, the exposures to and protections against crime will vary in places deferentially affected by the daily routine of distinct populations. Crime distributions are also related to the nature of the population's dynamics in terms of their social and economic heterogeneity [21–23]. As a result of policy restrictions or relaxations, the dynamic crime opportunities led by population interactions are naturally associated with the ebb and flow of urban human activity [24].

Some COVID-19-related studies using opportunity theory principles highlighted that specific crime trends are associated with populations intertwined with various types of urban characteristics. For example, Felson et al. [8] found that burglary experienced reductions at the early stage of the pandemic restriction period, and this was related to the land use types of residence in Detroit, USA. In addition, in a case study in Chicago, USA, Campedelli et al. [25] demonstrated that community population size was highly and stably related to property crimes (e.g., burglary, robbery). Estévez-Soto [13] further demonstrated the relationship between public transport usage represented by passenger numbers and several crime types (e.g., non-violent robbery) in Mexico City. Recently, Chen et al. [24] found stronger spatio-temporal associations between urban human activity and property crime (e.g., larceny theft) than with violent crime during the stay-at-home periods in San Francisco, USA. Using data from Lancashire, U.K., Halford et al. [14] identified the significant crime variations during COVID-19 (e.g., shoplifting, theft from

vehicle) through building an index called 'Mobility Elasticity of Crime' by considering the connection between mobility and crime. Similarly, Cheung and Gunby [26] also identified the correlation between mobility variations and property crime changes in New Zealand cities during the pandemic. In addition, Frith et al. [27] identified that different types of burglary declines were consistent with mobility changes and household occupancy levels in London boroughs.

Another theoretical approach taken in a handful of COVID-19-related studies uses social disorganisation theory (SDT), which explores the neighbourhood's/community's inability to preserve residents' common values and social controls [28,29]. Combined with opportunity theories, contemporary SDT studies have examined socioeconomic conditions, including income, education, housing, and population stability, and found them to be significantly associated with crime outcomes in places or neighbourhoods [30–32]. In the context of social or natural interruption (e.g., disasters, epidemic outbreaks), SDT approaches propose that crime would increase in vulnerable neighbourhoods as their residents are less able to maintain social control [33–35]. To date, like the aforementioned research on exploring explanatory/predictors in crime variations during the pandemic, limited COVID-19 and crime research have utilised SDT-related characteristics. The exceptions are Andresen and Hodgkinson [36] and Hodgkinson et al. [37]. The former identified that certain property crime drops (theft of/from vehicles) and assault increases were connected with social-disorganisation-based socioeconomic conditions in neighbourhoods in a case study from Vancouver, Canada. Similarly, the latter found that crime change is differentiated into different communities, and such variations are related to several SDT variables (income, immigrants) in Saskatoon, Canada.

In summary, opportunity theories (based on RAT and CPT) and SDT-related pandemic research have demonstrated that human routine activity dynamics and population characteristics are associated with crime heterogeneity in places/communities. Empirically, a minority of COVID-19 and crime studies have considered human activity at the city level or examined the static SDT explanatory aspects in communities, but these generally ignore the dynamic effects of human activity and the role of social disorganisation in the context of urban-neighbourhood-level crimes. In addition, limited crime studies in the pandemic context have examined the variation of local spatial relationships between the population's routine activities and property crimes within local neighbourhoods across different pandemic restriction and relaxation policies.

2.2. Geo-Tagged Big Data for Crime Analytics

In recent years, with people actively sharing their digital footprints in various forms, the proliferation of massive geo-tagged/-located big data sets reflecting dynamic human mobility/activity has enabled researchers to quantify and model human behaviours within urban environments in space and time [38–40]. Geo-tagged big data include call detail record (CDR) data and global positioning system (GPS) data, among other types [41,42]. CDR data are generated as a result of the mobile phone tower recording the connected mobile device based on calling, texting messages, or cellular data communication. So, the CDR data include the time of service response and the locations of the corresponding cell towers [43,44]. GPS data are recorded from mobile devices with location-based service enabled (LBS) when receiving signals. Unlike the CDR data providing the location information of fixed towers, GPS data offer the precise location coordinates and timestamps of an individual's movement trajectory points at a high resolution [39,45]. Besides, geo-tagged data on population mobility and activity can also be collected from various sources, such as survey data, transport smart card data, WiFi data, and social media data [46–49].

Empirically, the promises offered by geo-tagged/-located big data to crime research are prominently related to measuring the ambient population size or the population's human mobility/activity in urban areas. Bogomolov et al. [50] illustrated that the ambient population measured from the CDR users can discriminate between crime hot spots and other locations in urban areas. Similarly, Malleson and Andresen [51] utilised CDR data

and Twitter social media data to measure the ambient population and its impact on crime hotspots. Further, by measuring the local and non-local population (i.e., user numbers) from the CDR data set, Long et al. [52] used the ambient population as a proxy measure of guardianship and showed it significantly influenced offenders' target selection locations in robberies. He et al. [53] also found links between theft and the non-local ambient population with multiple demographic and activity features measured from aggregated CDR data. In addition, Hanaoka [54] showed a connection between street crime and the ambient population represented by users from aggregated GPS data. In terms of the mobility and activity measurement, Song et al. [55] quantified the relationship between theft target location and mobility flows of the ambient population measured from mobile phone CDR data. Also, Levy et al. [56] used Twitter social media data sets to measure residents' mobility and how it affects homicides. Using aggregated multi-source data sets (including subway and taxi usage data and mobile app data) to measure the human activity dynamics, Kadar and Pletikosa [57] demonstrated that spatio-temporal human activity can improve prediction performance in modelling several crime types, such as grand larceny and robbery.

Regarding COVID-19 and crime studies, limited analytical research has evaluated the impact of the dynamic population activity on crime patterns, excluding the reviewed works from Chen et al. [24] (based on SafeGraph data), Halford et al. [14], and Cheung and Gunby [26] (based on Google Community Mobility Reports), already reported in Section 2.1. Also, the insufficient previous research that examined the dynamic human activity's influence on crime patterns in neighbourhoods is related to the quality and extent of human activity data. For example, the 'Google Community Mobility Report' data (Google Community Mobility Report: https://www.google.com/covid19/mobility/, accessed on 1 February 2022) only provides the activity changes from the baseline in U.K. local authority (borough) areas. These are larger than the neighbourhood-level areas that are possible with the data used in the current analysis. Further, 'SafeGraph' data (SafeGraph: https://www.safegraph.com/, accessed on 1 February 2022) are currently not available for areas outside the U.S., which restricts the geographic scope of its use in analysis. Considering the alternative theoretical perspectives, there is now a need for empirical research based on geo-tagged big data and other neighbourhood characteristics to capture the relationships between human activities and crime patterns and disentangle the variable crime shifts in urban communities during the COVID-19 pandemic.

3. Data

Table 1 summarises the data sources used in this study. Our data include: (1) geographical boundary data (see Section 3.1); (2) police-recorded data (see Section 3.2); (3) socioeconomic data (see Section 3.3); (4) place data (see Section 3.4); and (5) mobile phone GPS trajectory data (see Section 3.5).

Table 1. A summary of the data sources.

Category	Fields Used	Description	Source
Geographical boundary data	LSOA ID; names; geographical information	Local super output area (LSOA) geographical polygon information for the U.K.	Office for National Statistics
Police-recorded data	Bicycle theft; burglary; criminal damage and arson; robbery; shoplifting; theft from a person; vehicle crime;	Police-recorded data of different crime types	data.police.uk

Table 1. *Cont.*

Category	Fields Used	Description	Source
Socioeconomic data	Residents; unemployment; rent social house; education above level 4 (higher education); young residents; own cars above 3	U.K. 2011 census with demographic and socioeconomic conditions (LSOA-level)	Office for National Statistics
Place data	Eating and drinking; public transport; stations and infrastructure; tourism; gambling; venues, stage, and screen; food, drink, and multi-item retail	Point of interest with latitude, longitude, and classifications	Ordnance survey
Mobile phone GPS data	Latitude, longitude, date/time	Mobile phone GPS trajectories	Location Sciences

3.1. Study Area and Unit of Analysis

With a population of over nine million in 2020, our study area—London—is the capital and largest metropolis of England and the United Kingdom. London has 32 local authority districts and 1 city district (City of London). At the local neighbourhood level, London has 4835 local neighbourhood areas, which are called lower super output areas (LSOAs), derived from the official census in the U.K. As the geographical unit of analysis in this study, LSOA geographical boundary data in London were downloaded from the Office for National Statistics (Office for National Statistics: https://www.ons.gov.uk/, accessed on 10 October 2022).

As COVID-19 spread in global cities, London's population continued to suffer from the virus, while the metropolis had the highest rate of confirmed cases in the U.K. As an emergency social distancing measure, the first national lockdown announced by the English government commenced on 23 March 2020, following a set of restrictions in the city, such as stay-at-home orders and the closure of public transport and non-essential business. With the pandemic ongoing over two years, restrictions were adjusted according to the infection rate, leading to the second national lockdown from 5 November 2020 to 4 December 2020 and the third national lockdown from 4 January 2021 to 8 March 2021.

3.2. London-Police-Recorded Data

London-police-recorded data were downloaded from the 'Metropolitan police service' section on the U.K. online police data portal (Data.police.uk: https://data.police.uk/, accessed on 10 October 2022). The data included each crime event with the corresponding spatial (latitude, longitude, LSOA index) and temporal (month and year) information. In this study, we selected seven types of property-related crimes in the form recorded in the police data: bicycle theft, burglary, criminal damage and arson, robbery, shoplifting, theft from a person, and vehicle crime. We also defined a category named 'All property crime', which was the total of these seven types added together. The analysis excluded several crime categories that are either related to violence or lack clear definitions: anti-social behaviour, drugs, possession of weapons, public order, robbery, violence and sexual offence, other crime, and other theft.

Due to the 'geomasking' (location anonymisation) technique implemented in the coordinates of the police-recorded data before open release, the LSOA is the lowest geospatial areal unit with promised spatial accuracy for aggregated counting [58]. Then, crime rates were calculated using the crime counts and the residential population (see the next section) for each LSOA in London.

3.3. Socioeconomic Data

Socioeconomic data (LSOA-level) from the latest and available census (2011) data set were downloaded from 'Office for National Statistics' (ONS) in the U.K. As the released census data consisted of many demographic and socioeconomic characteristics, we only considered the factors reflecting the social disorganisation at each LSOA (neighbourhood area), which was guided by theoretical considerations and previous studies with SDT and criminological research in London [50,59,60]. The chosen variables included the percentage of the population/household of each LSOA in 'unemployment', 'living in rented social housing', 'educated to level 4 and above (e.g., certificate of higher education)', 'owning 3 or more cars', and 'young residents aged 16–34'. To clarify, static socioeconomic conditions were used to represent the social disorganisation measurement in this analysis, as is traditionally the case, although it is acknowledged that the dynamic measurement of social disorganisation has been addressed in some recent research [56,61].

In addition, to use the most-accurate figures on populations, the residential population (including the proportion of young residents aged 16–34) for the LSOAs was generated from the estimated data sets (mid-2020 version) released by the ONS. The residential population map (see Figure A1 in Appendix A) shows an uneven distribution across the LSOAs in London. The average residential population of London LSOAs is 1861, while the maximum number of residents is 17,275 and the minimum is 585.

3.4. Place Data

Previous research has clearly demonstrated that certain place venues play a significant role in shaping crime patterns in urban areas, such as crime clusters or concentrations [19,62,63]. Empirical studies conducted in London have previously utilised point-of-interest (POI) data to analyse crime-generating venues in urban areas and examine their relationship with criminal activities. These include specific types of places like train stations, shopping centres, recreational facilities, pubs, and fast food venues [51,64,65], all of which we analysed in this study (see Table 1 and below).

Our place data for London, i.e., point of interest (POI) data, were provided by Ordnance Survey (Ordnance Survey: https://www.ordnancesurvey.co.uk/, accessed on 1 July 2022) and relate to the year 2020. According to the classification scheme (Ordnance Survey POI support: https://www.ordnancesurvey.co.uk/business-government/tools-support/points-of-interest-support, accessed on 1 July 2022), there are three levels of POI classification for describing the place name types in the data set, including 9 groups at the first level, 52 categories at the second level, and 600 classes at the third level. For example, the 'Accommodation, eating and drinking' group from the first level includes two categories: 'Accommodation' and 'Eating and drinking' in the second level. Then, the 'Eating and drinking' category (second-level) includes eight classes ('Banqueting and function rooms', 'Fish and chip shops', 'Cafes, snack bars and tea rooms', 'Internet Cafes', 'Fast food and takeaway outlets', 'Pubs, bars and inns', 'Fast food delivery services', 'Restaurants') in the third level.

We selected places in six POI categories (according to the previous studies mentioned above) based on the second level to represent crime generators in our study area. These were (1) eating and drinking, (2) public transport, stations, and infrastructure (we also incorporated 'bus transport' at the second level into this category), (3) tourism, (4) gambling, (5) venues, stage, and screen, and (6) food, drink, and multi-item retail. Then, the crime generator indices for these six types of places were measured by their actual numbers in each corresponding LSOA. In this analysis, we assumed that the LSOAs with more crime generators will have more crime opportunities at such micro places than other neighbourhood areas (LSOAs).

3.5. Mobile Phone GPS Trajectory Data

The anonymous mobile phone GPS trajectory data in London were collected from broadly mobility-related apps (e.g., navigation, route planning, outdoor sports) and were

provided by Location Sciences (Location Sciences: https://www.locationsciences.ai/, accessed on 3 January 2023) under GDPR compliance (Under the GDPR, anonymous mobile phone GPS data are considered personal data and must be collected, processed, and stored with explicit consent from the user, ensuring confidentiality and security, while providing them rights to access, rectify, and erase their data. This research was fully GDPR-compliant. For more details, visit the GDPR website: https://gdpr-info.eu/, accessed on 1 July 2022). The authors were granted permission to access and utilise anonymous mobile phone data for research analysis purposes.

The GPS trajectories were collected from apps with LBS, while users moved or stopped at places under the app user agreements. In this study, there were 1,979,081 users (about 22% of the total London resident population) in Greater London during the observed two years (2020 and 2021). As an abundant source of trajectories collected from a diverse range of apps and a significant proportion of user numbers in the London population, our GPS data set can provide a good representation for measuring human activity dynamics. It should be noted though that the data are ultimately a sample based on those phone users willing to share their location details. The use of this data set in producing human activity variables is described in the next section.

4. Methods

4.1. Generation of Human Activity Variables

4.1.1. Footfall Generation from GPS Trajectory

As raw mobile phone trajectory data consist of sequential position records with temporal information, a metric of human activity named *footfall* can be aggregated from stays detected based on GPS data in urban areas. When a single user spends some time at a location/place, this can be delineated as a stay/stop (known as 'stay points') [45,47].

In this study, the footfall-generation process shown in Figure 1 consisted of both stay detection and aggregation counting, respectively. First, stay detection aims to retrieve stays representing human activity from the sequence of raw GPS trajectory points. For one user's GPS trajectory records P, it can be denoted as:

$$P = p_0 \overset{\Delta d_0, \Delta t_0}{\rightarrow} p_1 \overset{\Delta d_1, \Delta t_1}{\rightarrow} \dots p_k \overset{\Delta d_k, \Delta t_k}{\rightarrow} \dots p_{m-1} \overset{\Delta d_{m-1}, \Delta t_{m-1}}{\rightarrow} p_m, k = 0, 1, 2 \cdots m \quad (1)$$

where Δd_k and Δt_k are the spatial distance (Euclidean) and time–distance between two consecutive GPS points (p_k and p_{k+1}). Then, the set of stays S, $S = \{s_0, s_1 \cdots s_k \cdots s_{n-1}, s_n\}$, $k = 0, 1, 2 \cdots n, n < m$ can be detected from the GPS records P using the stay-detection algorithm. In detail, two preset parameters are needed in the stay-detection algorithm: D_{max} (the maximum Euclidean distance that records a user's movement around a location position to generate a stay/stop) and T_{min} (the minimum time duration that the records keep stationary within the time distance to count as a stay/stop at the location) [66,67].

In this work, we set D_{max} and T_{min} at 50 m and 5 min, which allowed us to find some users' significant location visiting from GPS trajectories [68]. In other words, a stay is a user spending at least 5 min within a distance of a 50 m spatial radius.

Following this, we aggregated the numbers of stays to footfalls as the proxy of the human activity metric for a predefined geospatial unit (i.e., LSOA) and temporal units (i.e., hourly, daily) after the implementation of the stay-detection process. In other words, we generated the hourly (24 h a day) stay footfalls in 4835 LSOAs of London from 1 January 2020 to 31 December 2021.

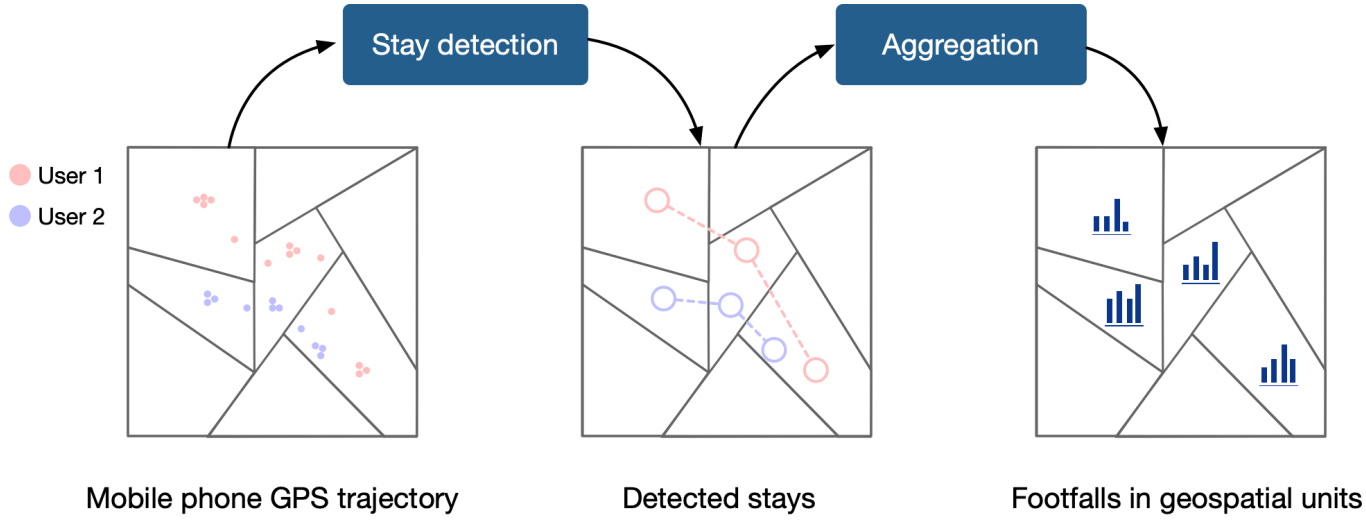

Figure 1. Footfall-generation process. The stay detection retrieves stays from different users' raw mobile phone GPS trajectories. Next, the footfalls in geospatial units are aggregated by the detected stays.

4.1.2. Characterising Dynamic Human Activity

To approximate aggregated urban daily dynamic routine, we characterised five daily routine time intervals for weekdays (WDs) and weekends (WEs) separately by measuring monthly daily average footfall (MDAF): early morning (0–6 h); morning (7–10 h); midday (11–15 h); afternoon (16–19 h); evening (20–23 h). The division of the 24 h day into five time intervals is a heuristic approach designed to characterise different daily routine patterns. Taking an approach that considers the likely patterns and routines of people at different times of the day is a common practice in the literature [69].

Taking the measuring MDAF of morning (WD) for a single LSOA for example, we first calculated the sum of footfalls from 7–10 h (the four hours are labelled as the 'morning' interval) in weekends across a month, then measured the daily average by dividing by the number of weekend days in that month. Thus, we obtained ten categories (five types of hourly intervals in a day for WDs and WEs) of dynamic human activity variables for 24 months for 4835 LSOAs in our study area.

4.2. Models

In this study, we aimed to train the LASSO regression model for eight types of property crime discriminated into three types of explanatory sets for comparisons (24 models in total). Specifically, the dynamic set denotes the human activity variables, and the static set denotes the social disorganisation and crime-generator variables. So, the models are named by the corresponding crime types with explanatory sets. For example, the burglary models with three types are static (S), dynamic (D), and static + dynamic (S + D).

4.2.1. LASSO Regression Model

To identify and compare the different impacts of dynamic human activity, social disorganisation, and crime generators on the crime pattern during the pandemic, we explored the relationship between property crime rates (eight types) and different explainable sets from the input explanatory variables (ten dynamic human activity variables, five static socioeconomic variables reflecting social disorganisation, and six place types reflecting crime generators) approached by LASSO regression models.

We utilised 'Least Absolute Shrinkage and Selection Operator' (LASSO) models [70] to conduct the empirical analysis due to the models' superiority in regression tasks as follows. First, as an improvement over the ordinary least-squares (OLS) model, the LASSO model implements a penalisation process (i.e., shrinking the coefficients with L_1 regularisation) on the explanatory variables (and setting some variables' coefficients to zero), thus highlighting the important explanatory variables for explaining the dependent variable. Second, the

LASSO model has the ability to process the data sets with multicollinearity, unlike the OLS model, which requires the independence of the explanatory variables [71]. Practically, the LASSO model has been used in various empirical criminological research papers due to its ability to identify important variables efficiently [72,73].

Mathematically, suppose we obtain p types of explanatory variables (independents) for the n response cases (dependent variables), i.e., explanatory matrix $\boldsymbol{X}$ $(p \times n)$ and response vector $\boldsymbol{y}$. Then, the cost function $\boldsymbol{J}$ of LASSO linear regression can be denoted as:

$$\boldsymbol{J} = \frac{1}{n}\sum_{i=1}^{n}(f(x_i) - y_i)^2 + \alpha \cdot \|\boldsymbol{\omega}\|_1, i = 1, 2, \cdots, n \tag{2}$$

where $\frac{1}{n}\sum_{i=1}^{n}(f(x_i) - y_i)^2$ is the cost function (mean-squared error) of OLS linear regression and $\|\boldsymbol{\omega}\|_1$ is the L_1 regularisation of coefficient vector $\boldsymbol{\omega}$, $\|\boldsymbol{\omega}\|_1 = \sum_j^p |\omega_j|, j = 1, 2, \cdots, p$. In addition, α is a constant that controls the degree of L_1 regularisation in the cost function $\boldsymbol{J}$. Then, we can tune the parameter α (as ω is subject to α) to obtain the optimised LASSO regression model by minimising the cost function $\boldsymbol{J}$.

4.2.2. LASSO Model Training Setup

Data preparation. For model training preparation, we first separated the data set into the training and testing sets following the '80/20' rule, which has been used elsewhere [74]. The training set included 19 months of data from January 2020 to July 2021 (approximately 80% of the data set), and the testing set included 5 months of data from August 2021 to December 2021 (approximately 20% of the data set). In other words, we split the data set ($\boldsymbol{X}$ and $\boldsymbol{y}$) into the training set ($\boldsymbol{X_{train}}$ and $\boldsymbol{y_{train}}$) for selecting the best LASSO model with the optimised parameter (α) and testing set ($\boldsymbol{X_{test}}$ and $\boldsymbol{y_{test}}$) for evaluating the model's performance.

Then, we performed z-score standardisation in the explanatory matrix $\boldsymbol{X_{train}}$ and $\boldsymbol{X_{test}}$, respectively. The z-score standardisation can be denoted as:

$$z_k = \frac{x_k - \mu}{\sigma}, \mu = \frac{1}{m}\sum_{k=1}^{m}(x_k), \sigma = \sqrt{\frac{1}{m}\sum_{k=1}^{m}(x_k - \mu)^2}, k = 1, 2, \ldots, m. \tag{3}$$

where x_k is an element of set $\{x_k\}$ equal to $\boldsymbol{X_{train}}$ or $\boldsymbol{X_{test}}$. μ and σ are the mean value and standard deviation of $\{x_k\}$, respectively.

Model training—parameter tuning. In the training set (19 months of data), we trained each LASSO regression model/regressor that estimates the regularisation parameter α through the k-fold cross-validation process. In detail, the k-fold cross-validation splits the training set into k parts with equal sizes. Then, in the k training times, each part of the data is used to validate the fit regression model with parameter α and test the error of the cost function (see Equation (2)). In this process, the coefficient vector $\boldsymbol{\omega}$ is estimated by the LassoCV algorithm (LassoCV: https://scikit-learn.org/stable/modules/generated/sklearn.linear_model.LassoCV.html, accessed on 10 March 2022) through minimising its cost function until small enough compared with a constant (i.e., α is determined). The α values were set to range from 0.001 to 1, with each value incrementing by 0.001. The range of 0.001 to 1 covers the most-commonly used alpha values for LASSO regressors, and the small increment (0.001) allows a fine-grained search for the optimal alpha value in the training process [75]. Finally, we selected the optimised α (corresponding to the minimised error) to develop the prediction LASSO model.

Model performance evaluation. For model evaluation, root-mean-squared error (RMSE) and coefficient of determination (R^2) were used as the two model performance metrics to evaluate the optimised LASSO models. First, the RMSE is defined as the root

value of the mean-squared errors (the mean-squared error is introduced as Equation (2)) between the predicted and the real/observed values. The RMSE can be denoted as:

$$RMSE = \sqrt{\frac{\sum_{k=1}^{l}(y_k - \hat{y_k})^2}{l}}, k = 1, 2, \cdots, l, l < m \tag{4}$$

where y_k is the true value in the testing set and $\hat{y_k}$ is the predicted value. l is the number of testing set samples. Second, R^2 is a correlation metric that represents the proportion of variance of predicted values that has been explained by the true values in the predictive model.

It can be denoted as:

$$R^2 = 1 - \frac{\sum_{k=1}^{l}(y_k - \hat{y}_k)^2}{\sum_{k=1}^{l}(y_k - \bar{y})^2}, \bar{y} = \frac{1}{l}\sum_{k=1}^{l} y_k, k = 1, 2, \cdots, l, l < m \tag{5}$$

where $\bar{y}$ is the mean of the true values. Hence, the lower the RMSE value and the higher the R^2, the better the performance of the trained LASSO models is. In this study, the performance evaluations were implemented using the training set (19-month data set) to generate predicted values and the testing set (5-month data set) as the true values for each respective model. To clarify, as the RMSE reflects the specific value difference, it can only be used for comparing the models with the same response variables (y_k), i.e., the same crime-type models.

4.2.3. Geographically Weighted Regression Model

Geographically weighted regression (GWR) is a local form of spatial regression that allows for the modelling of varying relationships across geospatial areas. Unlike the OLS model with the assumption of a stationary or a constant relationship throughout the study area, GWR allows for spatially varying relationships across the spatial units. In particular, while OLS regression provides a single equation to represent the relationship between the dependent and independent variables, GWR generates a unique regression equation for each observation in the data set based on its local neighbourhood [76].

GWR is an extension of the OLS model, formulated as:

$$y_i = \beta_0(u_i, v_i) + \beta_1(u_i, v_i)x_{i1} + \ldots + \beta_k(u_i, v_i)x_{ij} + \epsilon_i(u_i, v_i) \tag{6}$$

where y_i is the dependent variable, x_{ij} the independent variable for observation i, β_k the coefficient, and ϵ_i the error. In addition, (u_i, v_i) are the spatial coordinates of the observation. One of the most-important aspects of GWR is the weighting function, which ensures that observations closer to the location (u_i, v_i) have more influence on the local parameter estimates than those further away. A common choice for this function is the Gaussian function:

$$w_{ij} = \exp\left(-\frac{d_{ij}^2}{2s^2}\right) \tag{7}$$

where w_ij is the weight applied to observation j when estimating the parameters for observation i and d_{ij} is the distance between observations i and j. s is a bandwidth parameter that controls the rate of decline of the weights with increasing distance. GWR offers deeper insights into the data by identifying how different areas might deviate from the global trend, thereby offering a richer spatial context. This makes GWR particularly beneficial for examining the urban factors' relationship to crime across urban areas [77–79].

5. Results

5.1. Description of Explanatory Variables and Property Crime Rates

For an overview of the property crime and human activity variation, Figure 2 presents the footfalls (measured by the MDAF) and property crime rates (per LSOA) in London from 2020 to 2021. Overall, all property crime rates were strongly related to footfalls (Spearman

$R^2 = 0.82$, $p < 0.001$) with significant policy-influenced changes observed during the 24-month period. The footfall and crime rates both showed a significant reduction from March 2020 to April 2020 as the first U.K. national lockdown was announced on 23 March 2020. Though the crime rates and footfalls began to return to previous levels until September 2020, the two levels decreased once more to lower levels in the early months of 2021 as the restriction policy came back into force (e.g., second national lockdown and third national lockdown).

All the data were collected for or aggregated to the 4835 LSOAs in London, with the dynamic data spanning the 24 months of 2020 and 2021. Table 2 shows the descriptive statistics for the explanatory variables (static variables of social disorganisation, crime generators, and dynamic human activity variables) and the eight types of crime rates. The mean values of the dynamic human activity variables indicate that, as would be expected, the midday period of weekdays (WDs) was the busiest time interval (the MDAF was 39.35) compared to the evenings of weekends (WEs) with the lowest MDAF (7.09). Within the property crime types analysed, the highest mean value of the crime rate was for vehicle crime (1.04 per 1000 population) and the lowest mean value for bicycle theft (0.23 per 1000 population).

Table 2. Descriptive statistics of explanatory variables and crime rates.

Variables	Mean	Std	Min	Max
Static variables in social disorganisation (proportion)				
Unemployment	0.05	0.02	0.01	0.18
Rent social house	0.23	0.20	0.00	0.91
Education above level 4	0.37	0.15	0.08	0.84
Young residents 16–34	0.32	0.09	0.13	0.77
Own cars above 3	0.04	0.04	0.00	0.31
Static crime generators (proportion)				
Eating and drinking	6.28	18.37	0.00	792
Public transport, stations, and infrastructure	4.41	5.01	0.00	140
Tourism	0.69	3.78	0.00	164
Gambling	0.36	0.99	0.00	24
Venues, stage, and screen	0.28	1.39	0.00	50
Food, drink, and multi-item retail	3.69	5.89	0.00	115
Dynamic human activity variables (MDAF)				
Early Morning (WD *)	20.27	21.15	0.22	1607.55
Morning (WD)	30.38	63.12	0.15	9311.00
Midday (WD)	39.35	74.92	0.90	8923.10
Afternoon (WD)	25.18	55.32	0.36	7457.05
Evening (WD)	7.13	14.81	0.09	1337.10
Early Morning (WE *)	16.15	15.52	0.13	1302.11
Morning (WE)	18.44	27.46	0.00	2297.00
Midday (WE)	38.81	71.09	1.00	3222.44
Afternoon (WE)	20.07	40.68	0.37	2291.50
Evening (WE)	7.09	14.16	0.00	1014.56
Crime rate (per 1000 population)				
All property crime	3.30	5.76	0.00	462.98
Bicycle theft	0.23	0.71	0.00	45.02
Burglary	0.57	0.80	0.00	34.04
Criminal damage and arson	0.52	0.75	0.00	25.86
Robbery	0.24	0.69	0.00	44.26
Shoplifting	0.34	1.54	0.00	96.17
Theft from the person	0.35	2.66	0.00	321.70
Vehicle crime	1.04	1.17	0.00	39.46

* WD: weekday; WE: weekend.

Figure 2. All property crime and footfall monthly change (per LSOA) from 2020 to 2021.

5.2. Optimised LASSO Models for Property Crimes

To examine the impacts of dynamic human activity, static variables of social disorganisation and crime generators on each type of property crime's rates, 24 LASSO regression models (eight types of crime × three sets of explanatory variables) were trained using the training set (19 months from January 2020 to July 2021) and evaluated for prediction using the testing set (5 months from August 2021 to December 2021). In each model's learning process (introduced in Section 4.2.2), the parameter α was tuned by 10-fold cross-validation and selected at the lowest cost function error.

Table 3 shows the performance evaluation metrics (RMSE, R^2) and parameters (α) of the optimised LASSO models trained based on the training set (19 months of data). Generally, the performances of the 'S+D' models (the combination of static and dynamic variables) in each type of property crime were better than the 'S' or 'D' models in isolation in terms of the RMSE and R^2 metrics generated. It can also be observed that the best-performing model was the 'Theft from the person (S + D) model' with the highest R^2 (0.57), and the worst was the 'Vehicle crime (S + D) model' with the lowest R^2 (0.05) compared to the other property crime (S + D) models.

More specifically, the predictive power of the static explanatory variables (social disorganisation and crime generators) and dynamic variables (human activity) showed differential effects for different types of property crime. For example, the dynamic human activity variables imposed a stronger association with the theft from a person, shoplifting, and robbery as the R^2 in the 'Theft from the person (D)' model, 'Shoplifting (D)' model, and 'Robbery (D)' model was much higher (0.52, 0.36, 0.26) than in the corresponding 'S' models (0.31, 0.30, 0.22). On the contrary, by comparing the R^2 of the 'S' and 'D' models in the bicycle theft (0.26 vs. 0.19), burglary (0.10 vs. 0.07), criminal damage and arson (0.14 vs. 0.09), and vehicle crime (0.05 vs. 0.06) categories, it was clear that the dynamic human activity variables and static variables imposed similarly weak effects on these four crimes. This is interesting because the results showed a distinct separation between crimes where people or business assets are the targets and those where the target is mainly residential or unattended property.

In the testing set (5 months of data), the model evaluation metrics (RMSE and R^2) of the optimised LASSO models in Table 4 showed results consistent with those in Table 3—namely, that the dynamic human activity was strongly associated with specific property crimes (e.g., theft from a person). Similarly, while the other property crimes (i.e., bicycle theft, burglary, criminal damage and arson, vehicle crime) were associated with (influenced by) the static and dynamic variables, the effects were quite weak (low R^2 values).

Table 3. Performance evaluation (RMSE, R^2 in the training set) and parameters (α) of optimised LASSO models.

Optimised LASSO Models	S *			D *			S + D *		
	RMSE	R^2	α	**RMSE**	R^2	α	**RMSE**	R^2	α
All property crime	3.17	0.42	0.001	2.88	0.52	0.004	2.67	0.59	0.002
Bicycle theft	0.49	0.26	0.024	0.51	0.19	0.001	0.48	0.27	0.022
Burglary	0.66	0.10	0.004	0.67	0.07	0.002	0.66	0.11	0.007
Criminal damage and arson	0.61	0.14	0.001	0.62	0.09	0.001	0.60	0.15	0.001
Robbery	0.48	0.22	0.001	0.46	0.26	0.001	0.45	0.31	0.002
Shoplifting	0.99	0.30	0.002	0.95	0.36	0.002	0.91	0.42	0.001
Theft from the person	1.48	0.31	0.001	1.24	0.52	0.001	1.17	0.57	0.001
Vehicle crime	1.01	0.05	0.001	1.00	0.06	0.02	1.00	0.07	0.007

* S: static explanatory variable (N = 11); D: dynamic explanatory variable (N = 10); S + D: static and dynamic explanatory variables (N = 21).

Table 4. Performance evaluation (RMSE, R^2 in the testing set) of optimised LASSO models.

Optimised LASSO Models	S *		D *		S + D *	
	RMSE	R^2	**RMSE**	R^2	**RMSE**	R^2
All property crime	4.36	0.53	4.12	0.53	3.73	0.62
Bicycle theft	0.47	0.31	0.51	0.17	0.46	0.32
Burglary	0.62	0.14	0.64	0.08	0.62	0.14
Criminal damage and arson	0.60	0.21	0.63	0.14	0.60	0.21
Robbery	0.57	0.42	0.56	0.38	0.52	0.49
Shoplifting	1.04	0.37	1.03	0.37	0.97	0.45
Theft from the person	2.65	0.43	2.32	0.51	2.20	0.57
Vehicle crime	1.08	0.09	1.08	0.08	1.07	0.10

* S: static explanatory variable (N = 11); D: dynamic explanatory variable (N = 10); S + D: static and dynamic explanatory variables (N = 21).

To examine the specific variables that had a high impact on property crimes, we output the local coefficients (ω) of all property crime (S + D) models, shown as Figure 3. Most S + D model outcomes showed that the set of dynamic human activity variables contributed more-significant effects in the regression models than the static variables. In particular, the human activity (MDAF) at midday (weekdays) imposed a stronger positive influence on the crime rates than other variables in all crime models, except for the 'Vehicle, burglary and bicycle theft (S + D) models'. Considering the models' performance, the human activity variables as the main contributors were highlighted, while the static variables' coefficients shrunk to nearly zero in the model with the highest performance in terms of the R^2 (see theft from a person, shoplifting, and robbery). For theft from a person, shoplifting, and robbery, it can be observed that human activity in the morning (7–10 h weekdays) had a negative effect on the crime rate.

In summary, the results of our eight optimised (S + D) models demonstrated that a combination of human activity, social disorganisation, and crime generators can help improve the model's performance regarding the crime rate as the response variables. Importantly, the dynamic human activity variables ('midday (WD)' was identified as the most-impacted variable) were shown to have the main contribution to the three types of property crimes (theft from a person, shoplifting, and robbery). In addition, the dynamic

human activity variables had a lower influence than the static variables on the crime rate in bicycle theft and burglary across the board.

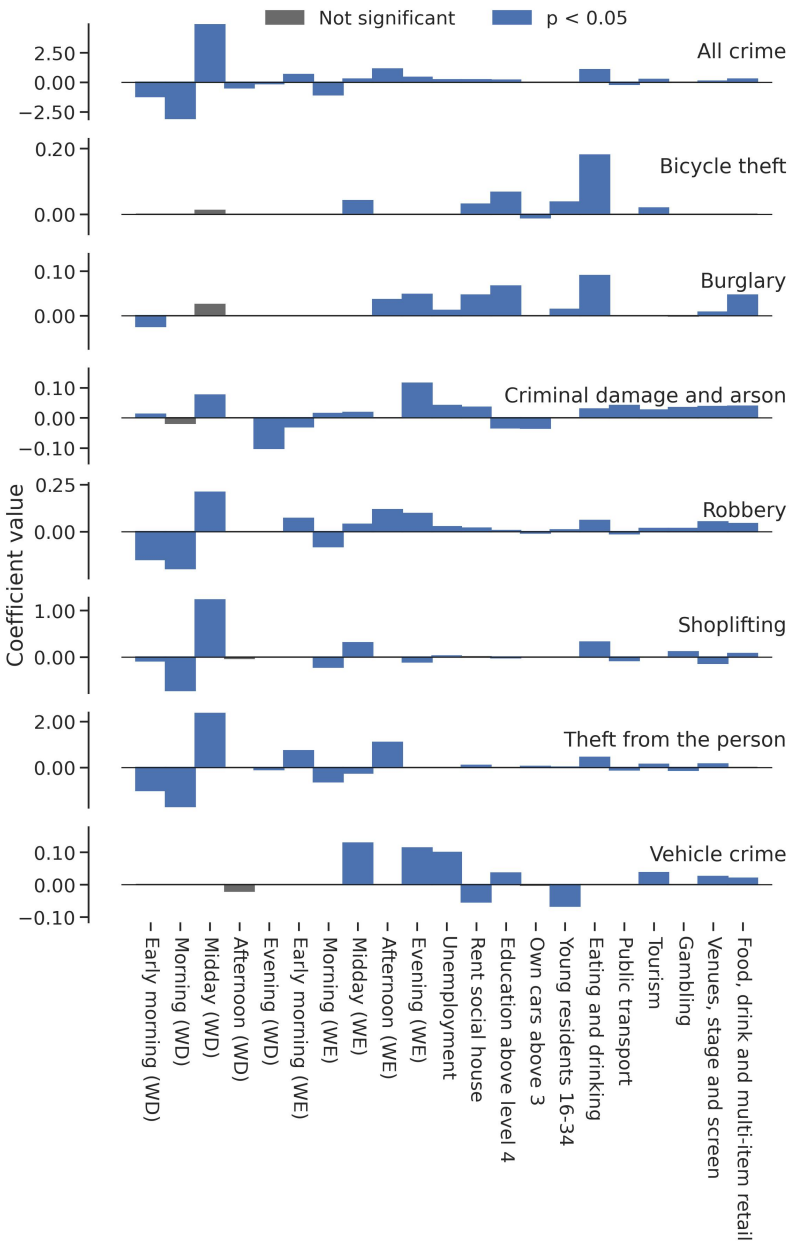

Figure 3. Standardised local coefficient values of explanatory variables in property crime (S + D) models. Each model's training set is 19 months of data from January 2020 to July 2021.

5.3. The Global Relationships between All Human Activity Variables and Theft in Four Pandemic Periods

To further explore how the time intervals of human activity influenced specific types of property crimes differed according to the rapid social change context, we investigated trends during the distinct pandemic periods. Thus, we chose to focus on particular types of crime, namely theft from a person and shoplifting, as they exhibited the strongest correlations (with $R^2 > 0.4$) with the human activity variables and other static factors in the long-term (S + D) models shown in Table 3. To clarify, as the most-significantly associated crime, a detailed examination of theft from a person is presented below, while the results of shoplifting are detailed in Appendix A to give the interested reader a further category for comparison.

This involved comparing four trained short-term (one-month) models reflecting the different restriction policies, which still considered all the alternative explanatory variables as our previous findings denoted that the S + D models reached the best performance (see Table 3). These four short-term 'Theft from the person (S + D) models' (see Figure 4) are labelled 'Before lockdown' model, 'First national lockdown' model, 'Lockdown easing' model, and 'Second national lockdown' model according to the related months (The first national lockdown was announced on 23 March 2020 and without amendments by the U.K. government on April 2020; several lockdown restrictions eased further in August 2020, including reopening indoor theatres and bowling alleys and 'Eating Out to Help out scheme'; the second national lockdown came in to force starting from 5 November 2020.). (i.e., February 2020, April 2020, August 2020, November 2020). The performance metrics (R^2) of the four optimised LASSO models (in the training set) were 0.75, 0.30, 0.60, and 0.53, demonstrating a better fit outside the lockdown periods, and the local coefficient values are also presented in Figure 4 (The results related to shoplifting can be seen in Figure A3 in Appendix A).

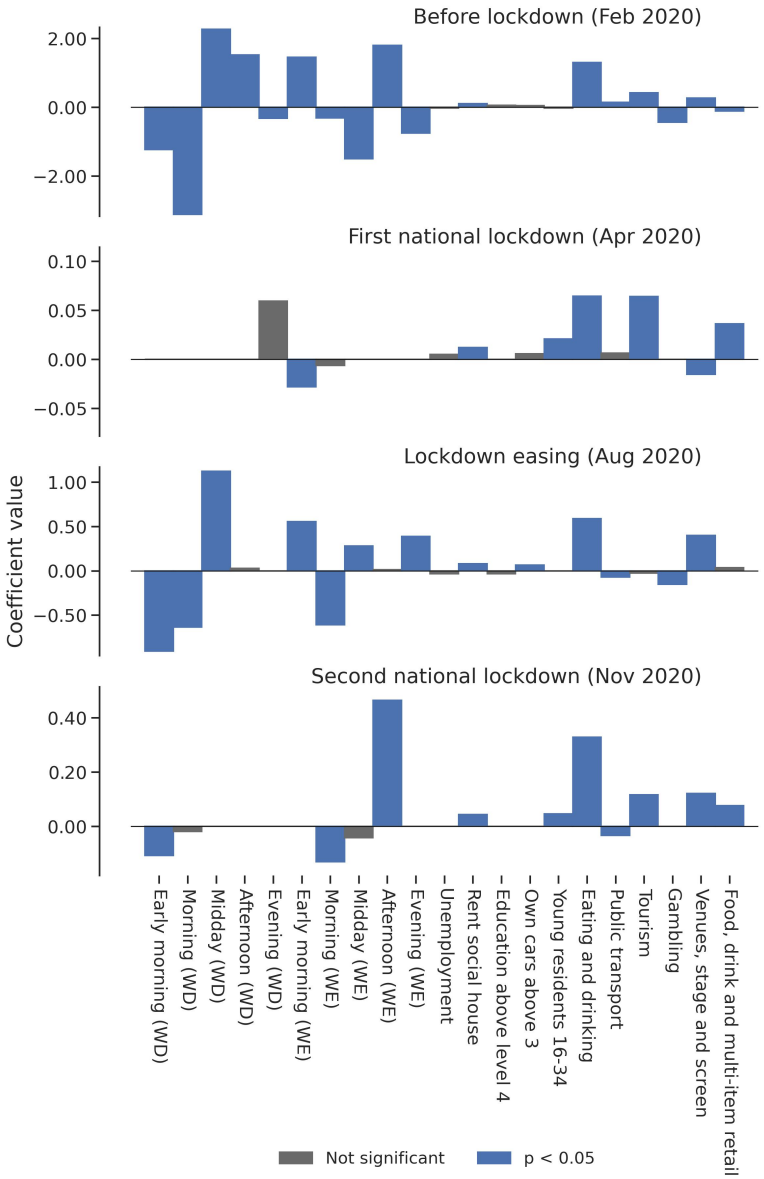

Figure 4. Standardised local coefficient values of explanatory variables in 'Short-term theft from a person (S + D) models'. Each model's training set is one month from January 2020, April 2020, August 2020, and November 2020, respectively.

Interestingly, these showed an uneven distribution in the distinct lockdown periods. That is, 'midday (WD)' had the highest (positive) coefficient value in both the 'Before lockdown' and 'Lockdown easing' models, but the highest values were for 'evening (WD)' (without statistical significance) in the 'First national lockdown' model and 'afternoon (WE) in the 'Second national lockdown' model. In other words, the results still demonstrated that the human activity level's impact on theft from a person varied in the four observed periods relating to the different restriction policies. Accordingly, the variations of the highest associated time intervals of human activity with the crime rate were in relation to the different restriction policies.

5.4. The Spatial Relationships between Selected Human Activity Variables and Theft in Four Pandemic Periods

Considering the spatial heterogeneity in human activity variations during the pandemic in our study area [80], we used geographically weighted regression (GWR) to test the spatial associations between the highest-performing activity variable and the risk of theft from a person for each distinct pandemic period. Following the results in the four LASSO regression models (see Figure 4), the human activity variables with a positive (>0) and the highest coefficient values were selected, i.e., 'midday (WD)' in the 'Before lockdown' model, 'evening (WD)' in the 'First national lockdown' model, 'midday (WD)' in the 'Lockdown easing' model, and 'afternoon (WE)' in the 'Second national lockdown' model. By mapping the local coefficient values of the selected human activity variables from the fit GWRs of four observation periods (shown in Figure 5), it became evident that the spatial distribution of the selected human activity's influence on theft from a person was affected by the restriction policies (The GWR results related to shoplifting can be seen in Figure A4 in Appendix A).

It is interesting to observe that the highly positive associations (mapped as dark red areas) were intertwined with the negative associations (mapped as dark blue areas) in the urban centres during normal times (i.e., before lockdown). Following the opportunity perspective, this mixed distribution indicates that population activities at midday on weekdays can generate crime opportunities or contribute to guardianship in different zones within urban areas. During the first national lockdown (April 2020), though the human activity volume and theft crime rate sharply decreased in all urban neighbourhoods, thefts in the urban centre remained highly associated with human activity. With human activity recovered by the lockdown easing period (August 2020), thefts driven by population activity at midday on weekdays were found in more widely distributed urban areas than before. Further, the associations in urban areas significantly differed between the first and second national lockdown periods, with the latter revealing more positively correlated areas.

Drilling down into the spatial distributions of the local coefficients in the GWRs revealed that contexts in terms of policies and restrictions mediated the relationship between theft and the human activity levels. We can also see from Figure 3 that the relationship between different types of property crime and the human activity in the areas appeared to vary both by the time of day or week and by the crime type. It is not insignificant that bicycle theft, vehicle theft, criminal damage, and burglary showed their own distinct patterns in these relationships. Neither is it insignificant that these varying and dynamic human activity levels were more powerful predictors than commonly used static explanatory variables for crime problems. This demonstrated that the relationships between populations undertaking activities and specific types of property crime are strong, supporting opportunity theories such as RAT, but it also demonstrated the need to consider the influence of the policy context and changes in the form of those activities and populations over the course of the day and week in shaping the nature of these relationships. It is clear that policing and prevention policies based on a 'more activity indicate more crime risk' principle is insufficiently nuanced.

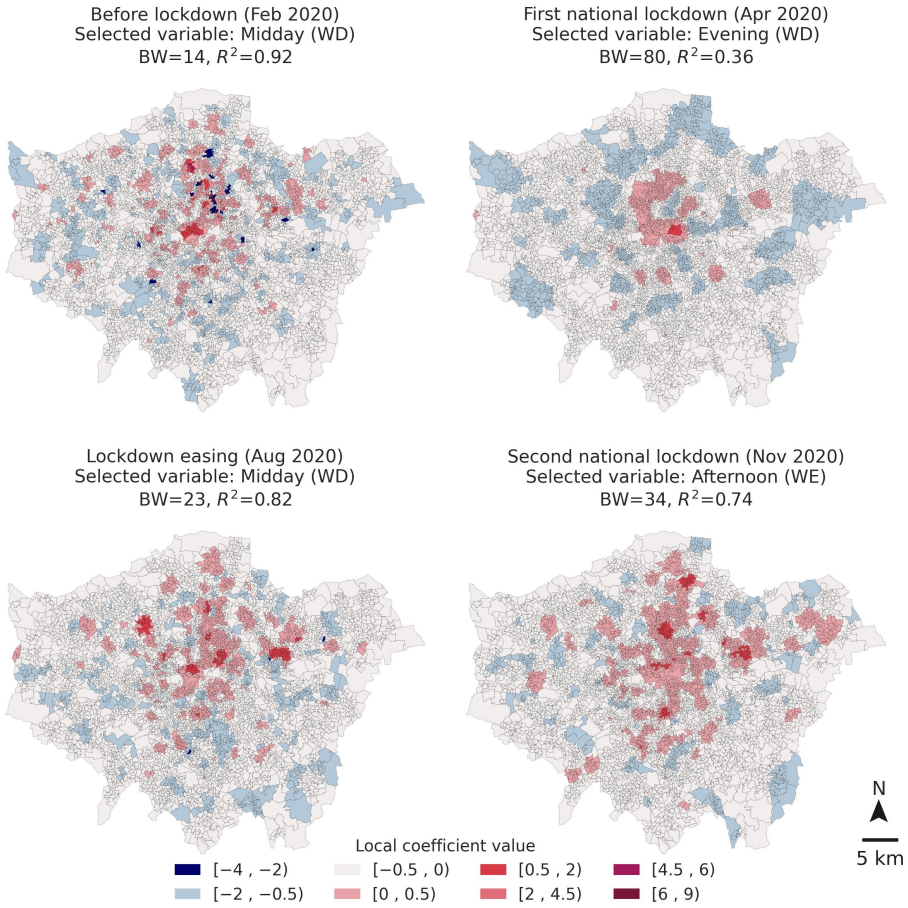

Figure 5. Maps of the spatial association (local coefficient values) between crime rates of theft from a person and the selected human activity variables in fit GWRs for February 2020, April 2020, August 2020, and November 2020. The bandwidths of the four GWRs are 14, 80, 23, and 34, respectively. The global R^2 of the four GWRs are 0.92, 0.36, 0.82, and 0.74, respectively.

6. Discussion

This study examined the impacts of dynamic human activity and static indicators of social disorganisation and crime generators on different types of crime rates in London during the COVID-19 period. Using geo-tagged big data (mobile phone GPS trajectory data set), the dynamic human activity variables were measured at the LSOA level for 24 monthly intervals separated into ten categories characterising daily and weekly population routines. Then, a series of models identified that dynamic human activity (especially the human footfall during lunchtime on weekdays) was particularly highly correlated with the rates of theft from a person, shoplifting, and robbery. These results can facilitate our understating of how human activity dynamics influenced property crime patterns during the pandemic. The findings reflect previous studies that have found associations between dynamic activity variables and property crimes for large spatial units of analysis. For example, they specifically reflect Estévez-Soto's [13] findings for non-violent robbery, Halford et al.'s [14] findings for shoplifting, and Chen et al.'s [24] findings for theft. The results also demonstrated that, particularly in some contexts, social disorganisation variables made explanatory contributions to variations in crime across the COVID-19 period, in keeping with the findings of Andresen and Hodgkinson [36].

The impacts of dynamic human activity were particularly strong for theft from a person, which is likely to be highly related to its Modus Operandi or mechanism. For theft from a person, the busier neighbourhoods (LSOAs in London) with a high human activity volume (i.e., footfall) reflect the population's visiting frequency, potentially generating more theft opportunities for offenders than the less-busy areas. Intuitively, the busier areas also

continually attract offenders who prefer more-targeted opportunities. Human activities in the midday of weekdays (11–15 h) were consistently found to be the busiest temporal interval during the 19-month training set (in terms of the highest mean of the MDAF; see Table 2) and also obtained the highest coefficient for theft opportunities compared to other time intervals. The findings that human activities in the mornings (i.e., morning (WD), morning (WE)) were found to be negatively related to theft risk appear to indicate that routine activities in different daily time intervals exhibit different guardianship levels and have different influences on theft. These patterns were also mirrored for robbery and shoplifting and support the idea that available populations can perform different risk and protective functions for property crime at different times of the day.

The findings from this research offer significant insights into theoretical and policy implications regarding property crimes. Theoretically, the results in this study align with the opportunity theories: the observed high correlation between routine activities and property crime incidences supports the notion that increased human activity creates more opportunities for crime. This analysis further develops the understanding of crime studies based on social disorganisation theory, highlighting how the interplay between dynamic human activities and static measurements of neighbourhood conditions can aid in disentangling the factors that influence crime rates.

In terms of policy implications, these findings can inform situational-crime-prevention strategies considering the variations of human routine activity patterns in urban areas. Authorities can concentrate on place management in areas with high footfall traffic, particularly during the busy periods identified through geo-tagged big data analysis. Intervention could involve increased police presence and improved surveillance focusing on particular crime types to alert potential victims during peak times in specific and manageable small urban areas. The variation in crime rates across different restriction and relaxation periods also suggests that crime prevention strategies need to be adaptable to changing circumstances in urban areas. Overall, this approach can assist in developing a dynamic and responsive crime prevention strategy that aligns with the fluctuating patterns of human activity.

The current research has several limitations. First, while the human activity measured by footfalls can reflect the overall association with the crime, such routine activity measurement neglects the semantic information of visiting behaviours (i.e., shopping, eating, or staying at home), so it cannot reveal how distinct types of human behaviour affects the specific type of crimes during the pandemic and beyond. In other words, further micro-level exploration is required to understand the role of guardianship as distinct from target availability in the interaction between places/activities, populations' mobility, and crime. An example would be if the ambient population, in sufficient density, is walking on the street, which might be a form of guardianship that reduces the risk of street crime, whereas if the ambient population is congregated at a bar at night, that might increase the risk of theft from vehicles in a parking lot. A further potential concern is the association between the GPS dynamic activity measures and the population denominators used to calculate crime rates. To investigate this, the relationships (R square) between the ten types of human activity variables and the resident population in the LSOAs were calculated (see Figure A2 in Appendix A). The resulting coefficients were statistically significant and showed some overlap. However, the R-squared values varied considerably between 0.1 and 0.75, demonstrating differences in strength over months and times of the day and confirming the distinction between these variables.

Second, due to the LASSO regression method, to a degree, the models highlighted the dynamic human activity variables by shrinking the static variable effects. Indeed, the coefficients of the variables in the LASSO models were more of a reference for the importance of certain features or variables relative to others. This means that the study cannot directly evaluate the absolute extent of the dynamic human activity variables in terms of their influence on crime.

Third, the measurement error associated with open police-recorded data varies across demographic groups and geographic areas due to the combined influences of victims'

under-reporting and police forces' under-recording [81]. Police data also have known issues with spatial uncertainty and spatial accuracy. Further, open source police data from the U.K. are geomasked to maintain privacy, which means that the location provided is only accurate on average to the nearest eight households [82].

Fourth, researchers have argued that the anonymous mobile phone GPS data may not fully represent the entire population [39,83]. This type of data is often sourced from users of specific apps or devices, which may exclude groups of the population who do not use or are rarely able to gain access to these services, such as older adults or lower-income individuals [84]. There are also sampling biases as to whom frequently uses mobile phones and whom allows their location data to be collected [85,86]. This bias suggests that the mobility patterns of certain groups might be disproportionately represented in analysing the relationships between routine activities and crime across urban areas. For example, in terms of evaluating the impact of routine activities on crime, certain areas would be under-represented due to the sample issues in population activities as measured by mobile phone GPS data.

7. Conclusions

In conclusion, this research analysed the impacts of dynamic human activity, static variables of social disorganisation, and crime generators on property crimes using the LASSO regression modelling in London-neighbourhood-level areas in the two-year period from 2020 to 2021. Dynamic human activity was identified as having the highest correlation with theft from a person amongst the other property crimes. In particular, human activity footfall in the midday of weekdays demonstrated the highest positive correlations with theft from a person. Further, the effects of the time intervals of human activity on theft from a person varied across restriction periods—with the highest association during normal times and the lowest during the first national lockdown period. Comparing theft from a person to other property crimes, there were obvious variations demonstrating distinct relationships between property crimes and activity levels at different times of the day and week. This demonstrated the need to consider the distinct influences of population activity changes over disparate times and contexts in determining the relationship between footfall and specific types of crime.

The pre-defined spatial and temporal units used in this research (e.g., the daily routine time intervals) are, of course, just one way of aggregating the data to enable analysis and will be subject to aggregation bias. Future works could consider measuring human activity variables with the high-resolution place and daily temporal information from the GPS trajectory data, e.g., the daily activity routine patterns at crime generators. Such micro-level analysis could explore the relationships between property crime opportunity patterns and distinct local populations. Further, it would be useful to capture the specific influence of travelling populations (e.g., commuting) on crime levels in the models. In addition, the complex correlations between variables could be understood further using spatio-temporal models to understand the associations between human activity and crime patterns in both time and space.

Author Contributions: Conceptualisation, Tongxin Chen, Tao Cheng and Kate Bowers; methodology, Tongxin Chen; software, Tongxin Chen; validation, Tongxin Chen, Tao Cheng and Kate Bowers; formal analysis, Tongxin Chen; investigation, Tongxin Chen, Tao Cheng, and Kate Bowers; resources, Tao Cheng; data curation, Tongxin Chen; writing—original draft preparation, Tongxin Chen; writing—review and editing, Tongxin Chen, Tao Cheng and Kate Bowers; visualisation, Tongxin Chen; supervision, Tao Cheng and Kate Bowers; project administration, Tao Cheng; funding acquisition, Tao Cheng and Kate Bowers. All authors have read and agreed to the published version of the manuscript.

Funding: This research was partially supported by the U.K. Economic and Social Research Council Consumer Data Research Centre (CDRC) under Grant ES/L011840/1. The second author is funded by the Economic and Social Research Council under the U.K. Research and Innovation open call on COVID-19 under Grant ES/V00445X/1.

Data Availability Statement: All experimental data and source code are available at https://doi.org/10.5281/zenodo.7839662 or https://github.com/tongxinchen/Human_Activity_Crime_London, accessed on 30 May 2023.

Conflicts of Interest: The authors declare no conflict of interest.

Abbreviations

The following abbreviations are used in this manuscript:

RAT	Routine activity theory
CPT	Crime pattern theory
SDT	Social disorganisation theory
CDR	Call detail record
GPS	Global positioning system
UK	United Kingdom
ONS	Office for National Statistics
LSOAs	Lower super output areas
POI	Point of interest
WD	Weekdays
WE	Weekends
MDAF	Monthly daily average footfall
LASSO	Least Absolute Shrinkage and Selection Operator
RMSE	Root-mean-squared error

Appendix A

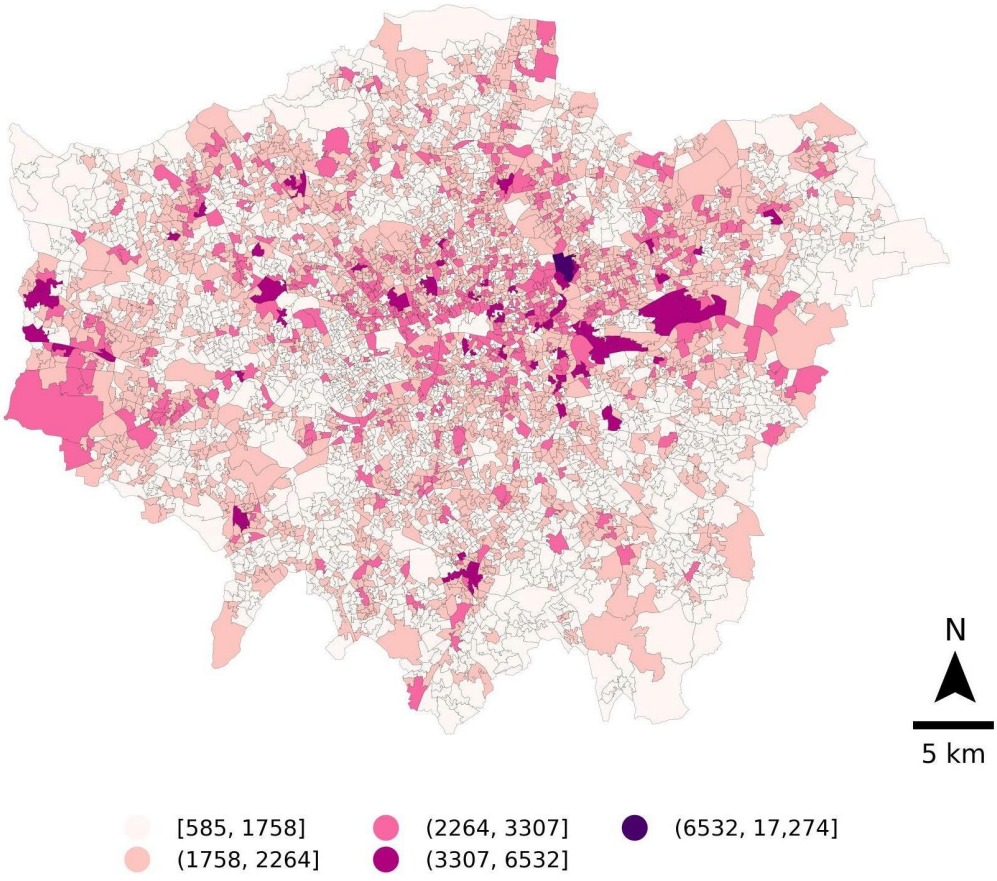

Figure A1. The map of the residential population in London LSOAs.

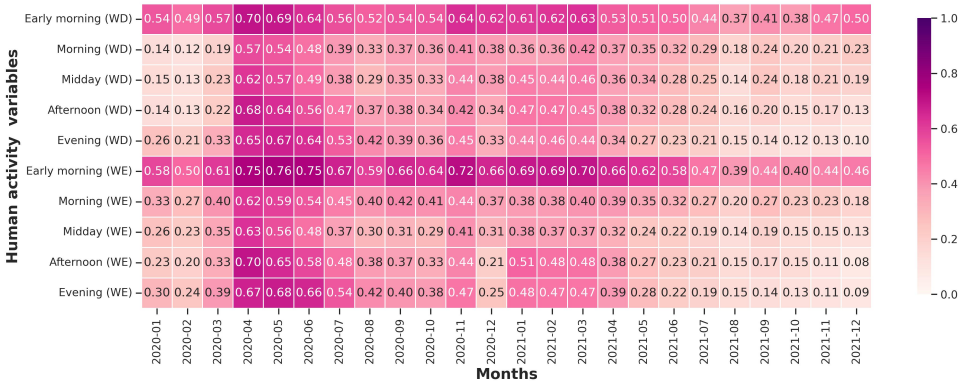

Figure A2. The relationship (R^2) between the ten types of human activity variables and resident population in LSOAs. The R-squared values were calculated from the fit OLS models (without constant) between the resident population and the dynamic human activity variables of the LSOAs during 24 months. All the p-values of the coefficients (human activity variables) are statistically significant ($p < 0.05$).

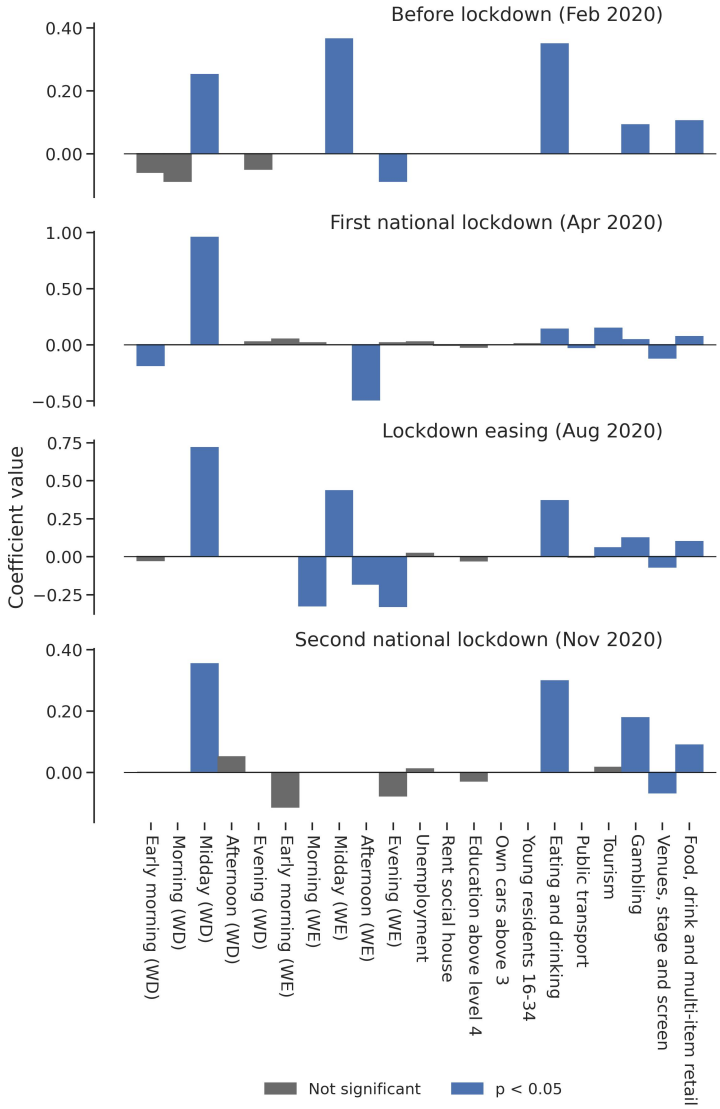

Figure A3. Standardisedlocal coefficient values of explanatory variables in 'Short-term shoplifting (S + D) models'. Each model's training set is one month from January 2020, April 2020, August 2020, and November 2020, respectively.

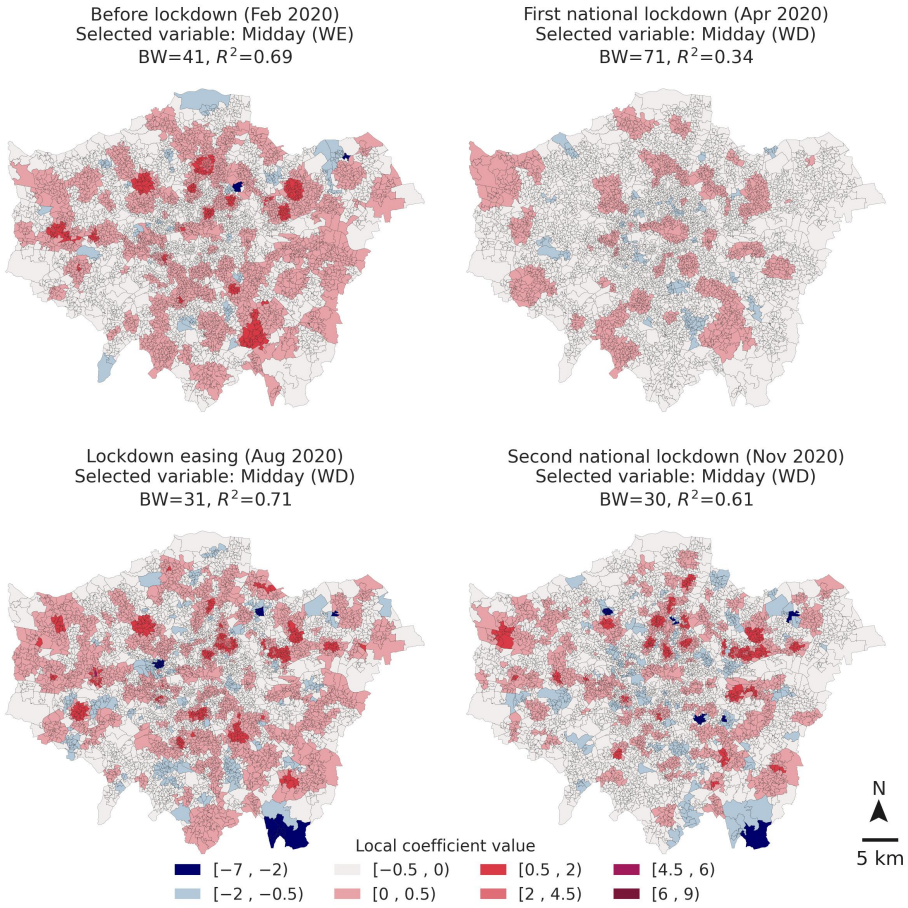

Figure A4. Maps of the spatial association (local coefficient values) between crime rates of shoplifting and the selected human activity variables in fit GWRs for February 2020, April 2020, August 2020, and November 2020. The bandwidths of four GWRs are 41, 71, 31, and 30, respectively. The global R^2 of four GWRs are 0.69, 0.34, 0.71, and 0.61, respectively.

References

1. Hale, T.; Webster, S.; Petherick, A.; Phillips, T.; Kira, B. Oxford COVID-19 government response tracker (OxCGRT). *Last Updat.* **2020**, *8*, 30.
2. Cheng, T.; Chen, T.; Liu, Y.; Aldridge, R.W.; Nguyen, V.; Hayward, A.C.; Michie, S. Human mobility variations in response to restriction policies during the COVID-19 pandemic: An analysis from the Virus Watch community cohort in England, UK. *Front. Public Health* **2022**, *10*, 999521. [CrossRef] [PubMed]
3. Ashby, M.P. Changes in police calls for service during the early months of the 2020 coronavirus pandemic. *Polic. J. Policy Pract.* **2020**, *14*, 1054–1072. [CrossRef]
4. Ashby, M.P. Initial evidence on the relationship between the coronavirus pandemic and crime in the United States. *Crime Sci.* **2020**, *9*, 6. [CrossRef] [PubMed]
5. Campedelli, G.M.; Aziani, A.; Favarin, S. Exploring the immediate effects of COVID-19 containment policies on crime: An empirical analysis of the short-term aftermath in Los Angeles. *Am. J. Crim. Justice* **2021**, *46*, 704–727. [CrossRef] [PubMed]
6. Langton, S.; Dixon, A.; Farrell, G. Six months in: Pandemic crime trends in England and Wales. *Crime Sci.* **2021**, *10*, 6. [CrossRef] [PubMed]
7. Mohler, G.; Bertozzi, A.L.; Carter, J.; Short, M.B.; Sledge, D.; Tita, G.E.; Uchida, C.D.; Brantingham, P.J. Impact of social distancing during COVID-19 pandemic on crime in Los Angeles and Indianapolis. *J. Crim. Justice* **2020**, *68*, 101692. [CrossRef]
8. Felson, M.; Jiang, S.; Xu, Y. Routine activity effects of the COVID-19 pandemic on burglary in Detroit, March, 2020. *Crime Sci.* **2020**, *9*, 10. [CrossRef]
9. Nivette, A.E.; Zahnow, R.; Aguilar, R.; Ahven, A.; Amram, S.; Ariel, B.; Burbano, M.J.A.; Astolfi, R.; Baier, D.; Bark, H.M.; et al. A global analysis of the impact of COVID-19 stay-at-home restrictions on crime. *Nat. Hum. Behav.* **2021**, *5*, 868–877. [CrossRef]
10. Balmori de la Miyar, J.R.; Hoehn-Velasco, L.; Silverio-Murillo, A. The U-shaped crime recovery during COVID-19: Evidence from national crime rates in Mexico. *Crime Sci.* **2021**, *10*, 14. [CrossRef]

11. Buil-Gil, D.; Zeng, Y.; Kemp, S. Offline crime bounces back to pre-COVID levels, cyber stays high: interrupted time-series analysis in Northern Ireland. *Crime Sci.* **2021**, *10*, 26. [CrossRef] [PubMed]
12. Koppel, S.; Capellan, J.A.; Sharp, J. Disentangling the impact of COVID-19: An interrupted time series analysis of crime in New York city. *Am. J. Crim. Justice* **2022**, *48*, 368–394. [CrossRef] [PubMed]
13. Estévez-Soto, P.R. Crime and COVID-19: Effect of changes in routine activities in Mexico City. *Crime Sci.* **2021**, *10*, 15. [CrossRef] [PubMed]
14. Halford, E.; Dixon, A.; Farrell, G.; Malleson, N.; Tilley, N. Crime and coronavirus: Social distancing, lockdown, and the mobility elasticity of crime. *Crime Sci.* **2020**, *9*, 11. [CrossRef] [PubMed]
15. Cohen, L.E.; Felson, M. Social Change and Crime Rate Trends: A Routine Activity Approach. *Am. Sociol. Rev.* **1979**, *44*, 588–608. [CrossRef]
16. Brantingham, P.J.; Brantingham, P.L. *Patterns in Crime*; Macmillan: New York, NY, USA, 1984.
17. Felson, M.; Cohen, L.E. Human ecology and crime: A routine activity approach. *Hum. Ecol.* **1980**, *8*, 389–406. [CrossRef]
18. Felson, M. The routine activity approach. In *Environmental Criminology and Crime Analysis*; Routledge: London, UK, 2016; pp. 106–116.
19. Brantingham, P.J.; Brantingham, P.L. The geometry of crime and crime pattern theory. In *Environmental Criminology and Crime Analysis*; Routledge: London, UK, 2016; pp. 117–135.
20. Brantingham, P.J.; Brantingham, P.L. Criminality of place: Crime generators and crime attractors. *Eur. J. Crim. Policy Res.* **1995**, *3*, 5–26. [CrossRef]
21. Sampson, R.J.; Raudenbush, S.W.; Earls, F. Neighborhoods and violent crime: A multilevel study of collective efficacy. *Science* **1997**, *277*, 918–924. [CrossRef]
22. Sampson, R.J.; Raudenbush, S.W. Systematic social observation of public spaces: A new look at disorder in urban neighborhoods. *Am. J. Sociol.* **1999**, *105*, 603–651. [CrossRef]
23. Sampson, R.J. Neighbourhood effects and beyond: Explaining the paradoxes of inequality in the changing American metropolis. *Urban Stud.* **2019**, *56*, 3–32. [CrossRef]
24. Chen, T.; Bowers, K.; Zhu, D.; Gao, X.; Cheng, T. Spatio-temporal stratified associations between urban human activities and crime patterns: A case study in San Francisco around the COVID-19 stay-at-home mandate. *Comput. Urban Sci.* **2022**, *2*, 13. [CrossRef] [PubMed]
25. Campedelli, G.M.; Favarin, S.; Aziani, A.; Piquero, A.R. Disentangling community-level changes in crime trends during the COVID-19 pandemic in Chicago. *Crime Sci.* **2020**, *9*, 21. [CrossRef] [PubMed]
26. Cheung, L.; Gunby, P. Crime and mobility during the COVID-19 lockdown: A preliminary empirical exploration. *N. Z. Econ. Pap.* **2022**, *56*, 106–113. [CrossRef]
27. Frith, M.J.; Bowers, K.J.; Johnson, S.D. Household occupancy and burglary: A case study using COVID-19 restrictions. *J. Crim. Justice* **2022**, *82*, 101996. [CrossRef] [PubMed]
28. Bursik, R.J., Jr. Urban dynamics and ecological studies of delinquency. *Soc. Forces* **1984**, *63*, 393–413. [CrossRef]
29. Sampson, R.J.; Groves, W.B. Community structure and crime: Testing social-disorganization theory. *Am. J. Sociol.* **1989**, *94*, 774–802. [CrossRef]
30. Jones, R.W.; Pridemore, W.A. Toward an integrated multilevel theory of crime at place: Routine activities, social disorganization, and the law of crime concentration. *J. Quant. Criminol.* **2019**, *35*, 543–572. [CrossRef]
31. Weisburd, D. The law of crime concentration and the criminology of place. *Criminology* **2015**, *53*, 133–157. [CrossRef]
32. Brantingham, P.J. Crime diversity. *Criminology* **2016**, *54*, 553–586. [CrossRef]
33. Prelog, A.J. Modeling the relationship between natural disasters and crime in the United States. *Nat. Hazards Rev.* **2016**, *17*, 04015011. [CrossRef]
34. Rumbach, A.; Makarewicz, C.; Németh, J. The importance of place in early disaster recovery: A case study of the 2013 Colorado floods. *J. Environ. Plan. Manag.* **2016**, *59*, 2045–2063. [CrossRef]
35. Tierney, K.; Bevc, C.; Kuligowski, E. Metaphors matter: Disaster myths, media frames, and their consequences in Hurricane Katrina. *Ann. Am. Acad. Political Soc. Sci.* **2006**, *604*, 57–81. [CrossRef]
36. Andresen, M.A.; Hodgkinson, T. In a world called catastrophe: The impact of COVID-19 on neighbourhood level crime in Vancouver, Canada. *J. Exp. Criminol.* **2023**, *19*, 487–511. [CrossRef] [PubMed]
37. Hodgkinson, T.; Andresen, M.A.; Frank, R.; Pringle, D. Crime down in the Paris of the prairies: Spatial effects of COVID-19 and crime during lockdown in Saskatoon, Canada. *J. Crim. Justice* **2022**, *78*, 101881. [CrossRef]
38. MacEachren, A.M. Leveraging big (geo) data with (geo) visual analytics: Place as the next frontier. In *Spatial Data Handling in Big Data Era*; Springer: Berlin/Heidelberg, Germany, 2017; pp. 139–155.
39. Barbosa, H.; Barthelemy, M.; Ghoshal, G.; James, C.R.; Lenormand, M.; Louail, T.; Menezes, R.; Ramasco, J.J.; Simini, F.; Tomasini, M. Human mobility: Models and applications. *Phys. Rep.* **2018**, *734*, 1–74. [CrossRef]
40. Jenkins, A.; Croitoru, A.; Crooks, A.T.; Stefanidis, A. Crowdsourcing a collective sense of place. *PLoS ONE* **2016**, *11*, e0152932. [CrossRef] [PubMed]
41. Haraguchi, M.; Nishino, A.; Kodaka, A.; Allaire, M.; Lall, U.; Kuei-Hsien, L.; Onda, K.; Tsubouchi, K.; Kohtake, N. Human mobility data and analysis for urban resilience: A systematic review. *Environ. Plan. Urban Anal. City Sci.* **2022**, *49*, 1507–1535. [CrossRef]

42. Toch, E.; Lerner, B.; Ben-Zion, E.; Ben-Gal, I. Analyzing large-scale human mobility data: A survey of machine learning methods and applications. *Knowl. Inf. Syst.* **2019**, *58*, 501–523. [CrossRef]
43. Brockmann, D.; Hufnagel, L.; Geisel, T. The scaling laws of human travel. *Nature* **2006**, *439*, 462–465. [CrossRef]
44. Mir, D.J.; Isaacman, S.; Cáceres, R.; Martonosi, M.; Wright, R.N. Dp-where: Differentially private modeling of human mobility. In Proceedings of the 2013 IEEE International Conference on Big Data, Silicon Valley, CA, USA, 6–9 October 2013; pp. 580–588.
45. Zheng, Y. Trajectory data mining: An overview. *ACM Trans. Intell. Syst. Technol. (TIST)* **2015**, *6*, 1–41. [CrossRef]
46. Alessandretti, L.; Sapiezynski, P.; Lehmann, S.; Baronchelli, A. Multi-scale spatio-temporal analysis of human mobility. *PLoS ONE* **2017**, *12*, e0171686. [CrossRef] [PubMed]
47. Zhao, K.; Tarkoma, S.; Liu, S.; Vo, H. Urban human mobility data mining: An overview. In Proceedings of the 2016 IEEE International Conference on Big Data (Big Data), Washington, DC, USA, 5–8 December 2016; pp. 1911–1920.
48. Pelletier, M.P.; Trépanier, M.; Morency, C. Smart card data use in public transit: A literature review. *Transp. Res. Part C Emerg. Technol.* **2011**, *19*, 557–568. [CrossRef]
49. Soundararaj, B.; Cheshire, J.; Longley, P. Estimating real-time high-street footfall from Wi-Fi probe requests. *Int. J. Geogr. Inf. Sci.* **2020**, *34*, 325–343. [CrossRef]
50. Bogomolov, A.; Lepri, B.; Staiano, J.; Oliver, N.; Pianesi, F.; Pentland, A. Once upon a crime: Towards crime prediction from demographics and mobile data. In Proceedings of the 16th International Conference on Multimodal Interaction, Istanbul, Turkey, 12–16 November 2014; pp. 427–434.
51. Malleson, N.; Andresen, M.A. Exploring the impact of ambient population measures on London crime hotspots. *J. Crim. Justice* **2016**, *46*, 52–63. [CrossRef]
52. Long, D.; Liu, L.; Xu, M.; Feng, J.; Chen, J.; He, L. Ambient population and surveillance cameras: The guardianship role in street robbers' crime location choice. *Cities* **2021**, *115*, 103223. [CrossRef]
53. He, L.; Páez, A.; Jiao, J.; An, P.; Lu, C.; Mao, W.; Long, D. Ambient population and larceny-theft: A spatial analysis using mobile phone data. *ISPRS Int. J. Geo-Inf.* **2020**, *9*, 342. [CrossRef]
54. Hanaoka, K. New insights on relationships between street crimes and ambient population: Use of hourly population data estimated from mobile phone users' locations. *Environ. Plan. B Urban Anal. City Sci.* **2018**, *45*, 295–311. [CrossRef]
55. Song, G.; Bernasco, W.; Liu, L.; Xiao, L.; Zhou, S.; Liao, W. Crime feeds on legal activities: Daily mobility flows help to explain thieves' target location choices. *J. Quant. Criminol.* **2019**, *35*, 831–854. [CrossRef]
56. Levy, B.L.; Phillips, N.E.; Sampson, R.J. Triple disadvantage: Neighborhood networks of everyday urban mobility and violence in US cities. *Am. Sociol. Rev.* **2020**, *85*, 925–956. [CrossRef]
57. Kadar, C.; Pletikosa, I. Mining large-scale human mobility data for long-term crime prediction. *EPJ Data Sci.* **2018**, *7*, 26. [CrossRef]
58. Tompson, L.; Johnson, S.; Ashby, M.; Perkins, C.; Edwards, P. UK open source crime data: Accuracy and possibilities for research. *Cartogr. Geogr. Inf. Sci.* **2015**, *42*, 97–111. [CrossRef]
59. Mburu, L.W.; Helbich, M. Crime risk estimation with a commuter-harmonized ambient population. *Ann. Am. Assoc. Geogr.* **2016**, *106*, 804–818. [CrossRef]
60. Sutherland, A.; Brunton-Smith, I.; Jackson, J. Collective efficacy, deprivation and violence in London. *Br. J. Criminol.* **2013**, *53*, 1050–1074. [CrossRef]
61. Browning, C.R.; Calder, C.A.; Soller, B.; Jackson, A.L.; Dirlam, J. Ecological networks and neighborhood social organization. *Am. J. Sociol.* **2017**, *122*, 1939–1988. [CrossRef] [PubMed]
62. Kinney, J.B.; Brantingham, P.L.; Wuschke, K.; Kirk, M.G.; Brantingham, P.J. Crime attractors, generators and detractors: Land use and urban crime opportunities. *Built Environ.* **2008**, *34*, 62–74. [CrossRef]
63. Bernasco, W.; Block, R. Robberies in Chicago: A block-level analysis of the influence of crime generators, crime attractors, and offender anchor points. *J. Res. Crime Delinq.* **2011**, *48*, 33–57. [CrossRef]
64. Belesiotis, A.; Papadakis, G.; Skoutas, D. Analyzing and predicting spatial crime distribution using crowdsourced and open data. *ACM Trans. Spat. Algorithms Syst. (TSAS)* **2018**, *3*, 1–31. [CrossRef]
65. Redfern, J.; Sidorov, K.; Rosin, P.L.; Corcoran, P.; Moore, S.C.; Marshall, D. Association of violence with urban points of interest. *PLoS ONE* **2020**, *15*, e0239840. [CrossRef]
66. Hariharan, R.; Toyama, K. Project Lachesis: Parsing and modeling location histories. In Proceedings of the International Conference on Geographic Information Science, Adelphi, MD, USA, 20–23 October 2004; Springer: Berlin/Heidelberg, Germany, 2004; pp. 106–124.
67. Pappalardo, L.; Simini, F.; Barlacchi, G.; Pellungrini, R. Scikit-mobility: A Python library for the analysis, generation and risk assessment of mobility data. *arXiv* **2019**, arXiv:1907.07062.
68. Yuan, N.J.; Zheng, Y.; Zhang, L.; Xie, X. T-finder: A recommender system for finding passengers and vacant taxis. *IEEE Trans. Knowl. Data Eng.* **2012**, *25*, 2390–2403. [CrossRef]
69. Tompson, L.; Bowers, K. A stab in the dark? A research note on temporal patterns of street robbery. *J. Res. Crime Delinq.* **2013**, *50*, 616–631. [CrossRef] [PubMed]
70. Tibshirani, R. Regression shrinkage and selection via the lasso. *J. R. Stat. Soc. Ser. B (Methodol.)* **1996**, *58*, 267–288. [CrossRef]
71. Tibshirani, R. Regression shrinkage and selection via the lasso: A retrospective. *J. R. Stat. Soc. Ser. B (Stat. Methodol.)* **2011**, *73*, 273–282. [CrossRef]

72. Chalfin, A.; Hansen, B.; Lerner, J.; Parker, L. Reducing crime through environmental design: Evidence from a randomized experiment of street lighting in New York City. *J. Quant. Criminol.* **2022**, *38*, 127–157. [CrossRef]
73. Wang, J.; Hu, J.; Shen, S.; Zhuang, J.; Ni, S. Crime risk analysis through big data algorithm with urban metrics. *Phys. A Stat. Mech. Its Appl.* **2020**, *545*, 123627. [CrossRef]
74. Hastie, T.; Tibshirani, R.; Friedman, J.H.; Friedman, J.H. *The Elements of Statistical Learning: Data Mining, Inference, and Prediction*; Springer: Berlin/Heidelberg, Germany, 2009; Volume 2.
75. Yang, L.; Shami, A. On hyperparameter optimization of machine learning algorithms: Theory and practice. *Neurocomputing* **2020**, *415*, 295–316. [CrossRef]
76. Fotheringham, A.S.; Charlton, M.E.; Brunsdon, C. Geographically weighted regression: A natural evolution of the expansion method for spatial data analysis. *Environ. Plan. A* **1998**, *30*, 1905–1927. [CrossRef]
77. Wheeler, D.C.; Waller, L.A. Comparing spatially varying coefficient models: A case study examining violent crime rates and their relationships to alcohol outlets and illegal drug arrests. *J. Geogr. Syst.* **2009**, *11*, 1–22. [CrossRef]
78. Bernasco, W.; Elffers, H. Statistical analysis of spatial crime data. In *Handbook of Quantitative Criminology*; Springer: Berlin/Heidelberg, Germany, 2010 ; pp. 699–724.
79. Jendryke, M.; McClure, S.C. Mapping crime–Hate crimes and hate groups in the USA: A spatial analysis with gridded data. *Appl. Geogr.* **2019**, *111*, 102072. [CrossRef]
80. Chen, T.; Zhu, D.; Cheng, T.; Gao, X.; Chen, H. Sensing dynamic human activity zones using geo-tagged big data in Greater London, UK during the COVID-19 pandemic. *PLoS ONE* **2023**, *18*, e0277913. [CrossRef]
81. Xie, M.; Baumer, E.P. Neighborhood immigrant concentration and violent crime reporting to the police: A multilevel analysis of data from the National Crime Victimization Survey. *Criminology* **2019**, *57*, 237–267. [CrossRef]
82. Kounadi, O.; Bowers, K.; Leitner, M. Crime mapping on-line: Public perception of privacy issues. *Eur. J. Crim. Policy Res.* **2015**, *21*, 167–190. [CrossRef]
83. Goodchild, M.F. The quality of big (geo) data. *Dialogues Hum. Geogr.* **2013**, *3*, 280–284. [CrossRef]
84. Marler, W. Mobile phones and inequality: Findings, trends, and future directions. *New Media Soc.* **2018**, *20*, 3498–3520. [CrossRef]
85. Snaphaan, T.; Hardyns, W. Environmental criminology in the big data era. *Eur. J. Criminol.* **2021**, *18*, 713–734. [CrossRef]
86. Rummens, A.; Snaphaan, T.; Van de Weghe, N.; Van den Poel, D.; Pauwels, L.J.; Hardyns, W. Do mobile phone data provide a better denominator in crime rates and improve spatiotemporal predictions of crime? *ISPRS Int. J. Geo-Inf.* **2021**, *10*, 369. [CrossRef]